ELSEVIER

Thermochimica Acta 367–368 (2001) 339–350

thermochimica acta

www.elsevier.com/locate/tca

Thermal characterization of organically modified montmorillonite

Wei Xie[a,*], Zongming Gao[a], Kunlei Liu[a], Wei-Ping Pan[a], Richard Vaia[b],
Doug Hunter[c], Anant Singh[d]

[a]*Thermal Analysis Laboratory, Material Characterization Center, Department of Chemistry,*
Western Kentucky University, Bowling Green, KY 42101, USA
[b]*AFRL/MLBP, Building 654, 2941 P Street, Wright-Patterson AFB, OH 45433, USA*
[c]*Southern Clay Products, Inc., 1212 Church Street, Gonzales, TX 78629, USA*
[d]*Triton Systems, Inc., 200 Turnpike Road, Chelmsford, MA 01824, USA*

Received 6 January 2000; accepted 1 June 2000

Abstract

Polymer/organically modified layered silicate (PLS) nanocomposites are a new class of filled polymers with ultrafine phase dimensions. They offer an outstanding combination of stiffness, strength and weight that is difficult to attain separately from the individual components. Additionally, the nanoscopic phase distribution as well as synergism between polymer and the layered silicate result in additional properties, such as flame retardency, enhanced barrier properties and ablation resistance, which are not observed in either component. These nanocomposites are synthesized by blending the organically modified layered silicate (OLS) into the polymer melt. Thus, understanding the relationship between the molecular structure and the thermal stability (decomposition temperature, rate, and the degradation products) of the organic modification of the layered silicate is critical. During this study, modern thermal analysis techniques combined with infrared spectroscopy and mass spectrometry (TGA–FTIR–MS) were used to obtain information on the thermal stability and degradation products. The effect of chemical variation (alkyl chain length, number of alkyls, and unsaturation) of organic modifiers on the thermal stability of the organically exchanged montmorillonite are discussed. A range of interesting results is observed, however, not all are currently understandable. © 2001 Elsevier Science B.V. All rights reserved.

Keywords: Organically modified layered silicate; Thermogravimetric analysis; Nanocomposites; Thermal stability

1. Introduction

Inorganic particles, such as talc, mica, carbon black and fumed silica, are widely used as reinforcement additives for polymers. At present, polymers reinforced by low weight percentages (1–10 wt.%) of nanoscopically dispersed organically modified layered silicates (OLS) are attracting the attention of government, academic and industrial researchers because of the unprecedented suite of new and enhanced properties relative to the unfilled resin. These polymer-layered silicate (PLS) nanocomposites are synthesized by blending the OLS into the polymer melt. The nanocomposite can attain a degree of stiffness, strength and barrier properties with far less

---

[*] Corresponding author. Tel.: +1-270-745-2665; fax: +1-270-780-2569.
E-mail addresses: wei-ping.pan@fsmail.wku.edu, wei-ping.pan@wku.edu (W.-P. Pan).

0040-6031/01/$ – see front matter © 2001 Elsevier Science B.V. All rights reserved.
PII: S0040-6031(00)00690-0

inorganic content than comparable glass- or mineral-reinforced polymers. Additionally, the nanoscopic phase distribution as well as synergism between polymer and the layered silicate result in additional properties, such as flame retardency, enhanced barrier properties and ablation resistance, which are not observed in either component [1].

OLSs have been known for more than 60 years [2–11]. They possess the same structural characteristics as the well-known minerals talc and mica (2:1 phyllosilicate) and are comprised of hydrated aluminum silicate. They are generally classified as clay minerals, which are the most abundant minerals on the surface of the earth. Their crystal structure consists of two-dimensional layers (thickness = 0.95 nm) formed by fusing two silica tetrahedral sheets with an edge-shared octahedral sheet of either alumina or magnesia [12]. Stacking of these layers leads to van der Waals' gaps or galleries. The galleries (alternatively referred to as interlayers) are occupied by cations, typically Na^+ and/or Ca^{2+}, which balance the charge deficiency that is generated by isomorphous substitution within the layers (e.g. tetrahedral Si^{4+} by Al^{3+} or octahedral Al^{3+} by Mg^{2+}). Because these cations are not structural they can be easily replaced by other positively charged atoms or molecules, and are called exchangeable cations [13]. In contrast to pristine-layered silicates containing alkali metal and alkali earth charge-balancing cations, OLSs contain alkyl ammonium or phosphonium cations [1,14]. The presence of these organic-modifiers in the galleries renders the originally hydrophilic silicate surface, organophilic. Depending on the functionality, packing density and length of the organic modifiers, the OLSs may be engineered to optimize their compatibility with a given polymer.

When preparing clay/polymer nanocomposite using either in situ polymerization or melt intercalation, a certain temperature is needed in the processing. If the processing temperature to make the PLS is higher than the thermal stability of the organic treatment on the OLS, some decomposition will take place. The onset temperature of decomposition of the organic treatment, therefore, is meaningful in the process to make a

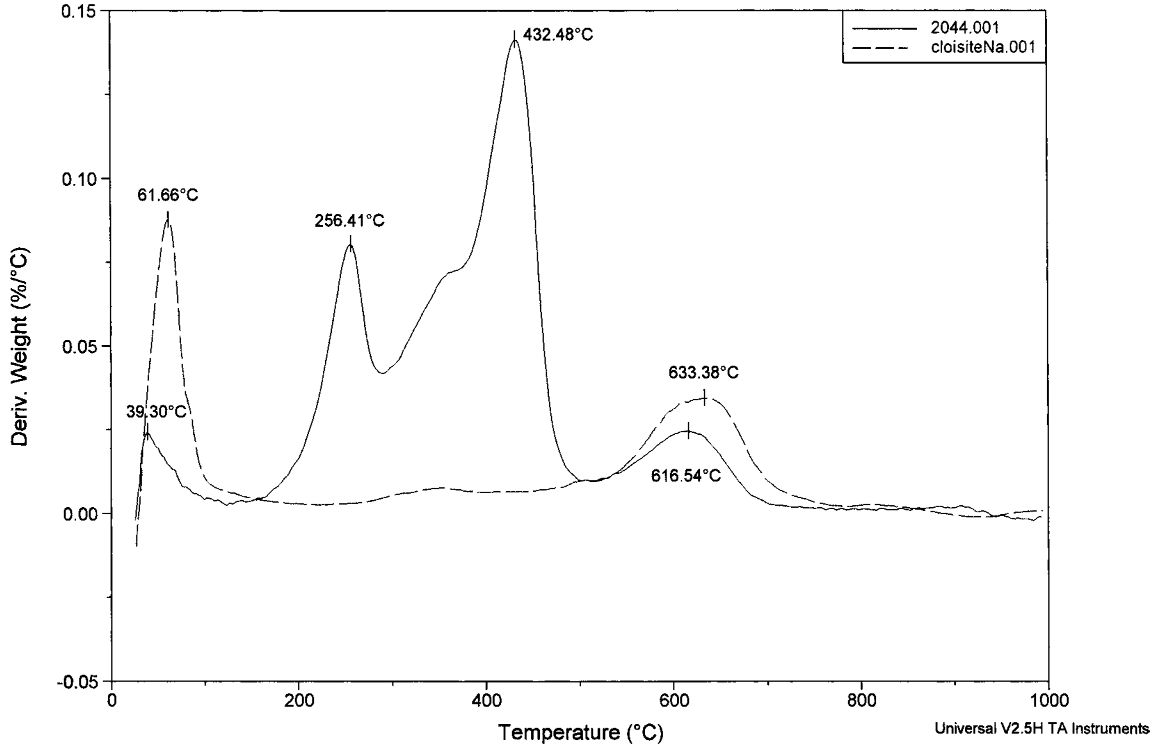

Fig. 1. Comparison of TGA curve of OLS 2044 and Na^+ montmorillonite.

Table 1
The summary of the major species evolved from each decomposition step of samples

Sample ID	Step 1 (<200°C)	Step 2 (200–500°C)	Step 3 (500–800°C)	Step 4 (800–1000°C)
Montmorillonite	Free water	CO_2, interlayer H_2O	Water from dehydroxylation CO_2	CO_2
2044	Free water	Organic water, CO_2, long-chain alkyl fragments	Water from dehydroxylation CO_2	Water, CO_2
2045	Free water	Organic water, CO_2, long-chain alkyl fragments	Water from dehydroxylation CO_2	Water, CO_2
2046	Free water	Organic water, CO_2, long-chain alkyl fragments	Water from dehydroxylation CO_2	Water, CO_2
2047	Free water	Organic water, CO_2, long-chain alkyl fragments	Water from dehydroxylation CO_2	Water, CO_2

clay/polymer nanocomposite. However, little is understood about the thermal stability of organo-clays while making nanocomposites. Therefore, it is necessary to study the thermal stability, fine structure, and the evolution of gaseous species of organo-clay complexes to establish the thermal stability and degradation mechanisms of OLSs. TGA/FTIR/MS is an outstanding technique to examine the above problem. In this study, the thermal degradation of organically modified montmorillonites was investigated and compared with pure montmorillonite. Modern thermal analysis techniques combined with infrared spectroscopy and mass spectrometry (TGA–FTIR–MS) were used to examine the effect of chemical variation (alkyl

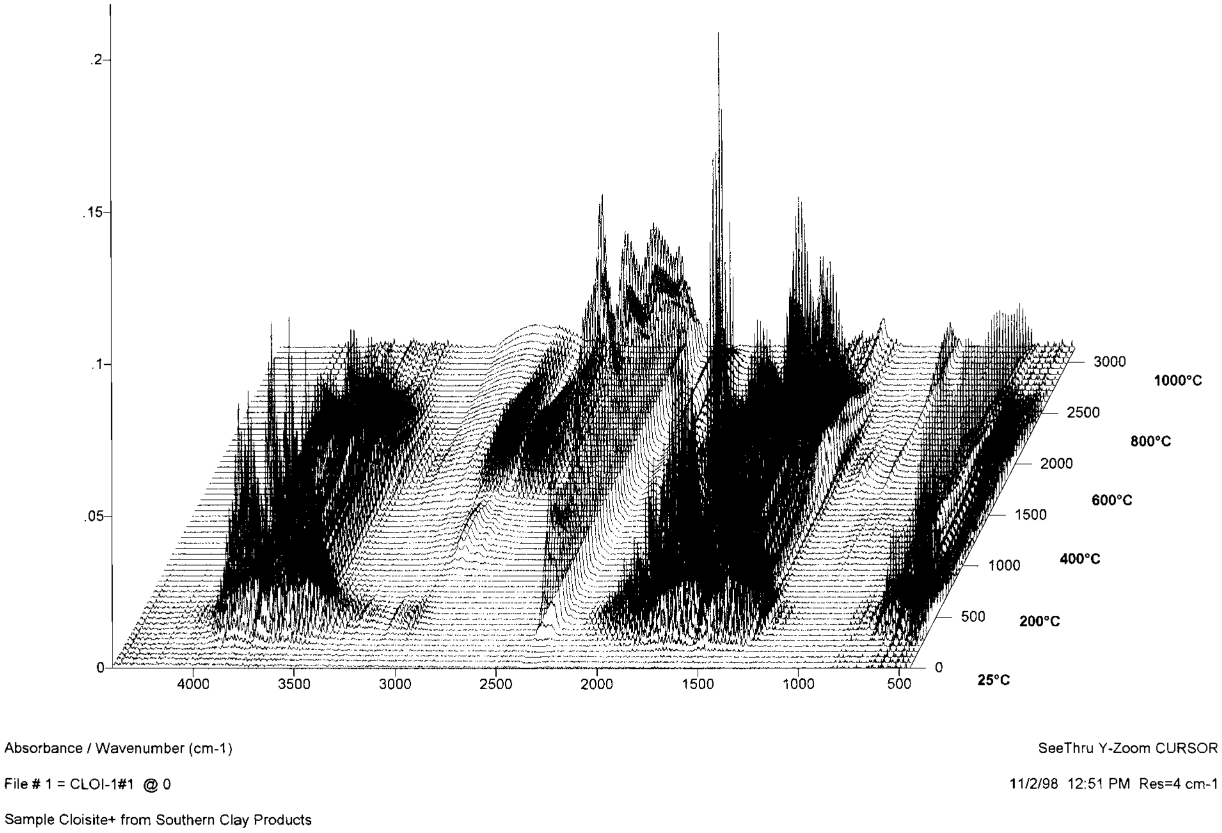

Fig. 2. 3D spectra of gases from Na^+ montmorillonite at a heating rate of 20°C/min.

chain length, number of alkyls, and unsaturation) of the organic modifiers on the thermal stability and degradation products of the organically modified montmorillonite.

2. Experimental

A number of montmorillonite and organically modified montmorillonite samples (2044, 2046, 2047, 2048) were examined. Pristine montmorillonite is the Na^+ exchanged. Sample 2044 is a montmorillonite exchanged with trimethylcoco, quaternary ammonium chloride; sample 2046 is a montmorillonite exchanged with trimethyltallow, quaternary ammonium chloride; sample 2047 is a montmorillonite exchanged with trimethyldodecyl, quaternary ammonium chloride; and sample 2048 is a montmorillonite exchanged with trimethyloctadecyl, quaternary ammonium chloride. Both tallow and coco are the mixture with $C_{16–18}$, and $C_{12–16}$ as the main components, respectively. Southern Clay Products supplied the experimental samples for this study.

2.1. *TG/MS technique*

An approximately 20 mg sample was placed in a ceramic pan and analyzed on an SDT (simultaneous TGA and DTA) 2960 interfaced to a Fisions VG Thermolab Mass Spectrometer by means of a heated capillary transfer line. The Fisions unit is based on quadrupole design with a 1–300 amu mass range. The sample gas from the interface was ionized at 70 eV. The system operates at a pressure of 1×10^{-6} Torr. The samples were heated at 20°C/min from room temperature to 1000°C in dynamic nitrogen atmosphere. The DTA

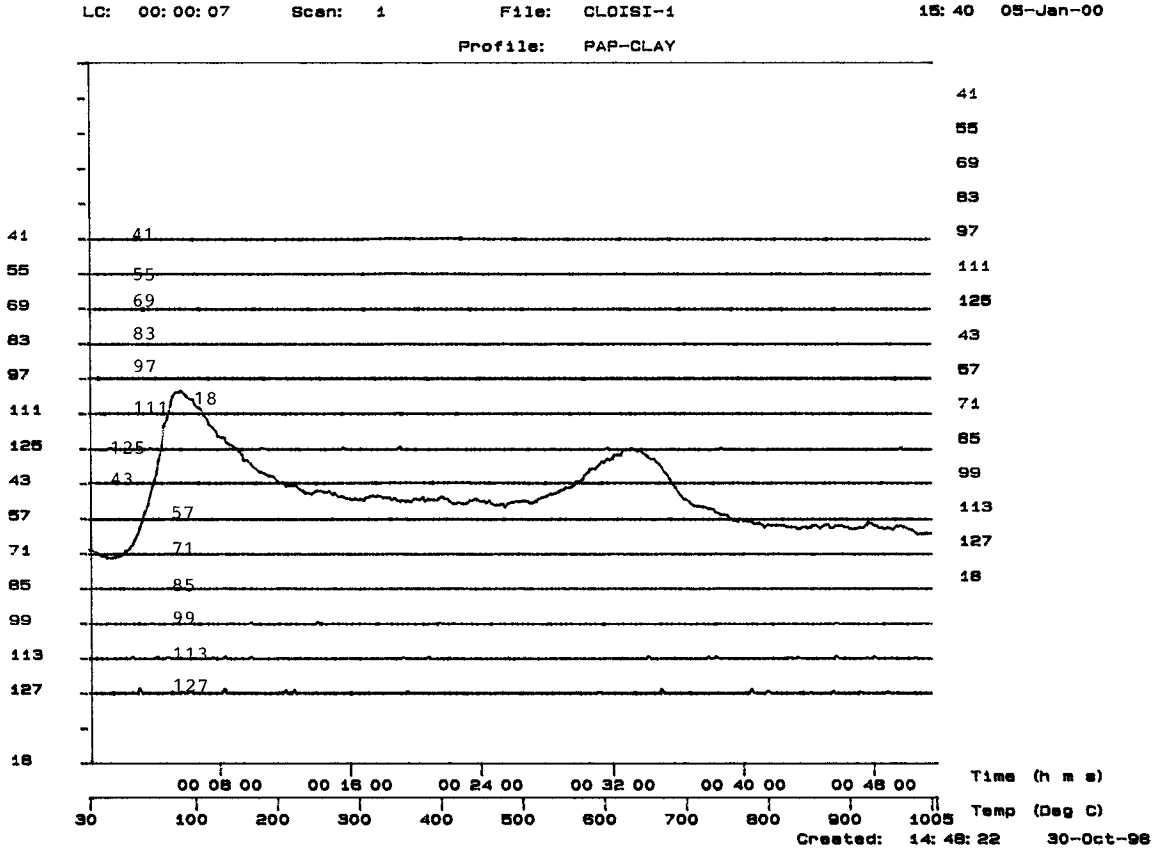

Fig. 3. MS profiles on gases from Na^+ montmorillonite at a heating rate of 20°C/min.

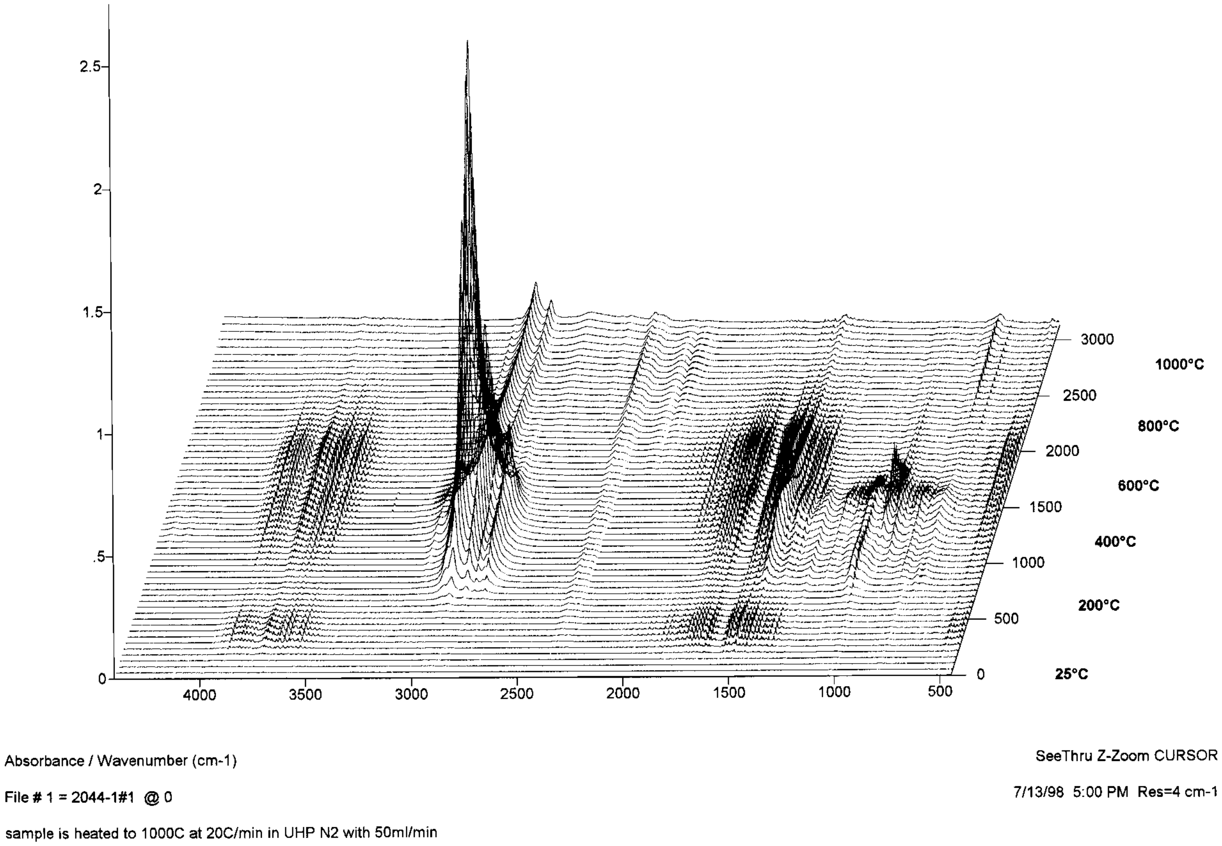

Fig. 4. 3D spectra of gases from OLS 2044 at a heating rate of 20°C/min.

reference was 20 mg of pure aluminum oxide. An NIST library database was used for MS analysis.

2.2. *TG/FTIR technique*

An approximately 50 mg sample was placed in the ceramic boat, and was heated in the TGA 951 at 20°C/min from ambient temperature to 1000°C, under a flowing (50 ml/min) nitrogen (UHP grade). The Dupont 951 TGA interfaced to a Perkin Elmer 1600 series FTIR with a permanent silicon transfer line (length 1 in.). The purge gas carries the decomposition products from the TGA through a 70 ml sample cell with KBr crystal windows. For detection of the decomposition products, the cell was placed in the IR scanning path and kept at 150°C by wrapped heating tape to prevent possible condensation. The IR detection range was 450–4500 cm^{-1}.

3. Results and discussions

The thermal decomposition of the organically modified montmorillonite (2044) will be discussed and compared to pristine sodium montmorillonite. Subsequently, the thermal decomposition of various organic cations will be compared to establish an understanding of structure property relationships.

3.1. *Thermal degradation of sodium montmorillonite and organically modified montmorillonite (2044)*

Initially consider the relative differences in the thermal decomposition of sodium montmorillonite and montmorillonite that has been exchanged with trimethylcoco, quaternary ammonium chloride (2044). Greene-Kelly [15] considered the montmorillonite differential thermal curve in two parts: (a) the free water and interlayer water region in the temperature range 100–300°C; (b) the structural water (bonded OH that undergoes dehydroxylation) region in the temperature range 500–1000°C. The DTGA thermal curve shown in Fig. 1 for the OLS is more conveniently considered in four parts: (1) the free water region in the temperature below 200°C; (2) the region where organic substances evolve in the temperature range 200–500°C; (3) the structural water region in the temperature range 500–800°C; (4) a region between 800 and 1000°C where organic carbon reacts in some yet unknown way. The major species evolved from each decomposition step are summarized in Table 1.

3.1.1. The loss of free and interlayer water

The large internal surface of montmorillonite leads to the naturally occurring minerals being highly hydrated and hence releasing free water (water between particles and sorbed on the external surfaces of crystals) before 100°C. Water in the interlayer space is gone when the temperature reaches 300°C. Greene-Kelly [12] found by X-ray measurements that over this temperature range the (0 0 1) spacing decreases from about 15 Å for Ca-saturated, or 11–12.5 Å for Na-saturated, samples to 9.5 Å and that no further decrease occurs at higher temperature. He concluded, therefore, that in this temperature range the bulk of the water is lost from the interlayer space. Again, water, as the main evolution product over this temperature range, has been confirmed by both TG–MS $(m/e = 18)$ and TG–FTIR (wave number $= 1300$–$1800\,\mathrm{cm}^{-1}$) results as shown in Figs. 2–5 during experiments.

Two distinct types of interlayer water are present in natural montmorillonite. Type (I) constitutes the inner

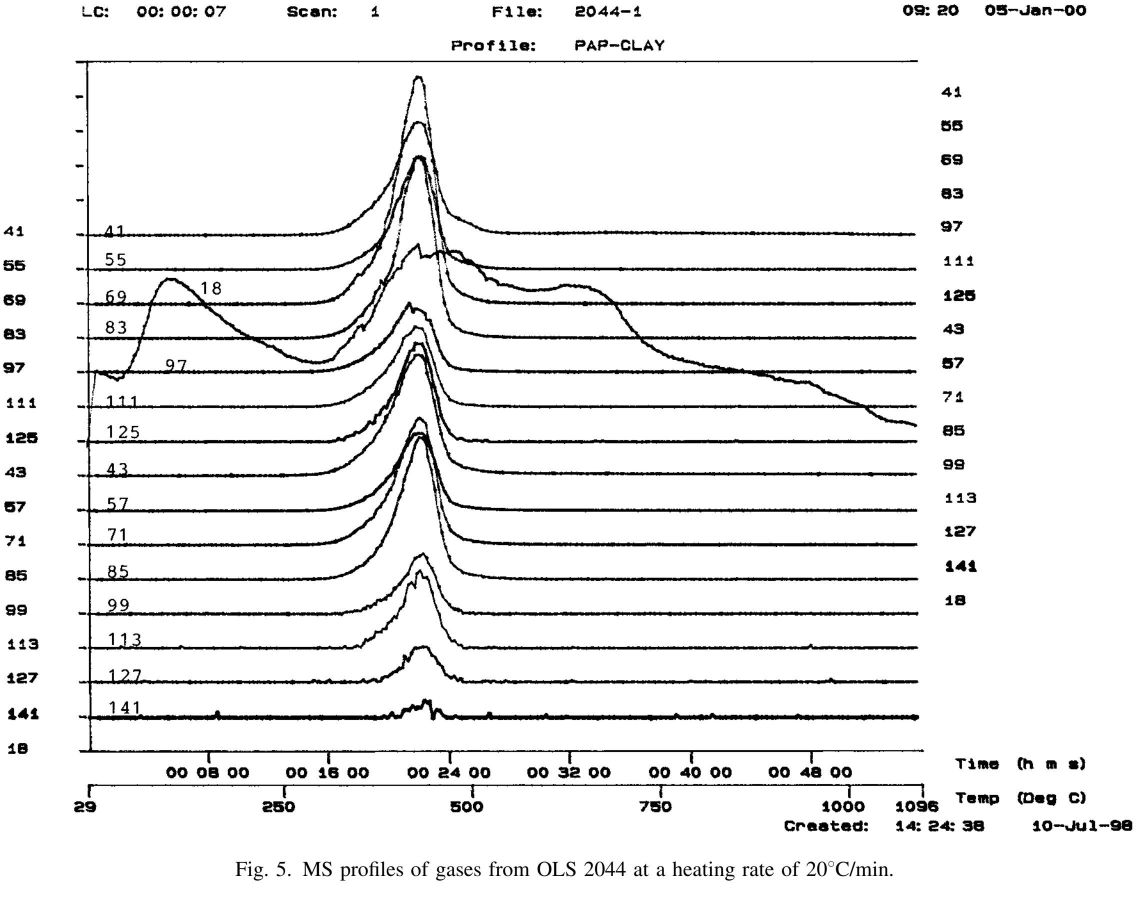

Fig. 5. MS profiles of gases from OLS 2044 at a heating rate of 20°C/min.

(primary) hydration shell around the exchangeable cation, i.e. the water which is directly coordinated to the cation; it gives a maximum absorption near 3600 and 1630 cm^{-1}. Type (II) forms the outer (secondary) coordination sphere of the cation; being indirectly linked to the cation and possessing greater mobility; it gives a spectrum similar to that shown by liquid water with a broad, strong OH stretching band near 3400 cm^{-1} and weaker H–O–H bending maximum near 1630 cm^{-1} [16,17]. The absorption at 3690 and 3620 cm^{-1} shown in the FTIR spectrum are due to hydroxyl group in the general formula for silicate structure.

The OLS samples, as demonstrated by sample 2044, have a different behavior than sodium montmorillonite. For sample 2044, the free water (~1%) disappears by 40°C. There is no interlayer water in the OSL as the quaternary ammonium salt has been exchanged for the hydrated sodium cation. The free and interlayer water (total ~4%) start evolving about 90°C for pristine sodium montmorillonite, but are not completely gone until about 300°C.

3.1.2. The organic substances evolving region in the temperature range 200–500°C

The most distinguished difference between the sodium montmorillonite and the organically modified montmorillonite is in the temperature range 200–500°C. The organic constituent in the organo-clay start to decompose somewhere above 200°C, which can be supported from the MS and FTIR spectrum (shown in Figs. 3 and 5). There are three overlapping DTGA peaks for sample 2044, which may reveal that the release of organic substances is from different mechanisms. The all four OLS samples used in this study have three DTGA peaks in this temperature

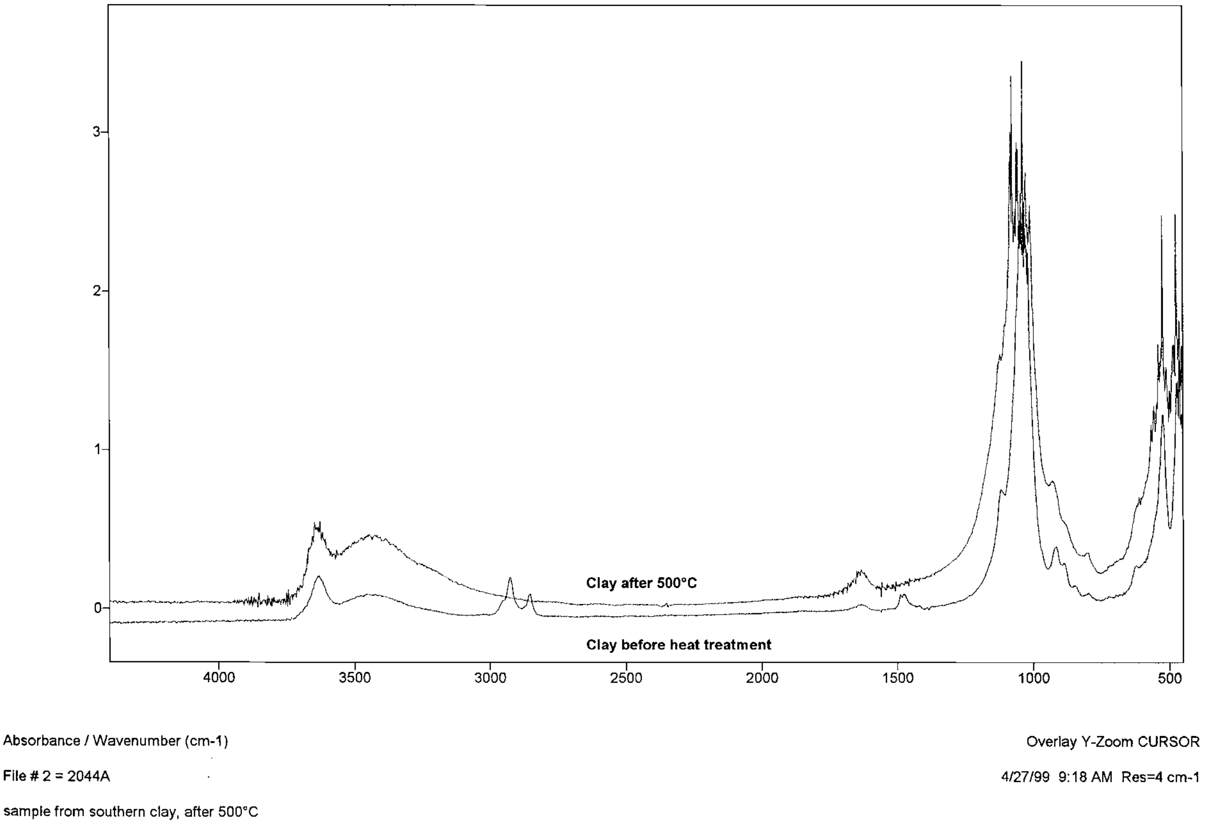

Fig. 6. Comparison of IR spectra of OLS 2044 with and without heat treatment.

range which indicates that the trimethylalkyl quants would have the same decomposition mechanism. Details about the evolution of organic substance will be discussed later.

In order to confirm that organic substances decomposed over the temperature range 200–500°C, sample 2044 was pyrolyzed from room temperature to 500°C, and then both the control sample 2044 and pyrolyzed sample were examined by FTIR. It is clearly shown in Fig. 6 that the organic C–H vibrations $(\text{wave number} = 2629, 2853, \text{and } 1478\,\text{cm}^{-1})$ disappeared after samples were heated to 500°C. Meanwhile, there were still OH absorption $(\text{wave number} = 3690, 3620, \text{and } 1636\,\text{cm}^{-1})$ [16,17] for the pyrolyzed samples that did not change in either frequency or intensity. It can be concluded, therefore, that the main weight losses over the temperature range 200–500°C are due to the decomposition of organic compounds.

3.1.3. The dehydroxylation region in the temperature range 500–800°C

In the temperature range 500–800°C, the hydroxyl group, which is covalantly incorporated in the crystal lattice, is dehydrated. The dehydration reactions in natural montmorillonite has been well investigated [18–20]. For sample 2044, water is again the decomposition product in this temperature range as confirmed by TGA–MS results shown in Fig. 5.

3.1.4. The high temperature reaction between organic carbon and inorganic oxygen between 800 and 1000°C

One of the most distinguishing differences between sodium montmorillonite and the organically modified montmorillonite is in the temperature range from 800 to 1000°C. Sodium montmorillonite is very stable when the temperature is higher than 800°C, however, the OLS continues to lose weight. Larger amount of

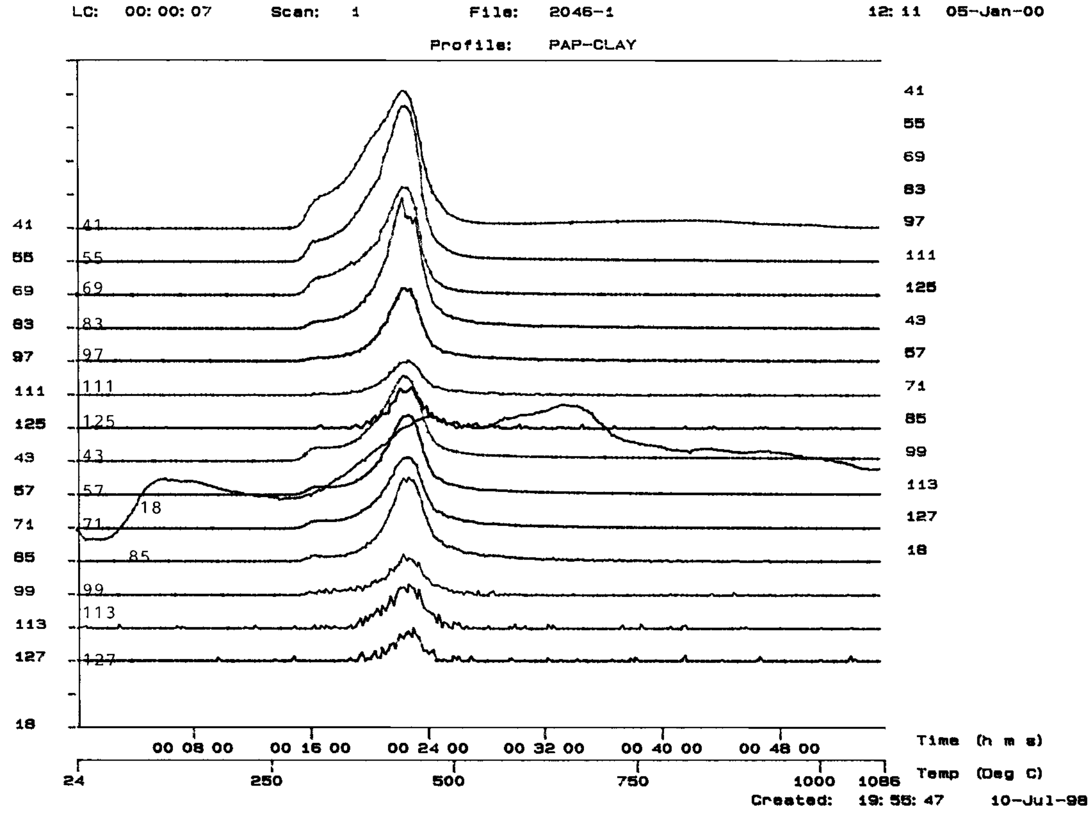

Fig. 7. MS profiles of OLS 2046 at a heating rate of 20°C/min.

CO_2 is released at temperature over 800°C. The pathway of the formation of CO_2 could be stated as following. The onium ion decomposition products, including alkanes, alkenes, were partially absorbed on the surface of the alumino-silicate. Subsequently, the absorbed organic was catalyzed by the alumino-silicate to CO_2 and/or the high temperature reaction of the carbon in the organic with the oxygen in the crystal structure of the montmorillonite.

3.2. The decomposition products and thermal stability of organically modified clay

The decomposition temperature of OLSs is a key processing factor since polymer processing is normally in excess of 150°C. Thus, processing of the nanocomposite as well as the initial melt blending of the OLS and polymer is near the thermal limits of the organic modifiers. In addition to common detrimental aspects of degradation, the resulting products may play a major and yet to be determined role in the formation of the exfoliated nanostructure. The quaternary ammonium ion is nominally chosen to compatiblize the layered silicate with a given polymer resin. However, the molecular structure, such as alkyl chain length, number of alkyls, and unsaturation, is also the determining factor of the thermal stability of the OLS. The effect of alkyl chain length, saturation and mixture on the thermal stability of the OLS is discussed.

Clearly, the decomposition product is a mixture of alkanes and alkenes. The release of alkanes and alkenes (as shown in Figs. 5, 7–9) can be identified from the MS spectra of the investigated materials $(m/z = 41, 55, 69, 83, 97, 111, 125, 139$, and $m/z = 43, 57, 71, 85, 99, 113, 127, 141)$. However, due to the limitation of detection of high molecular weight compounds, the Pyrolysis-GC/MS technique is

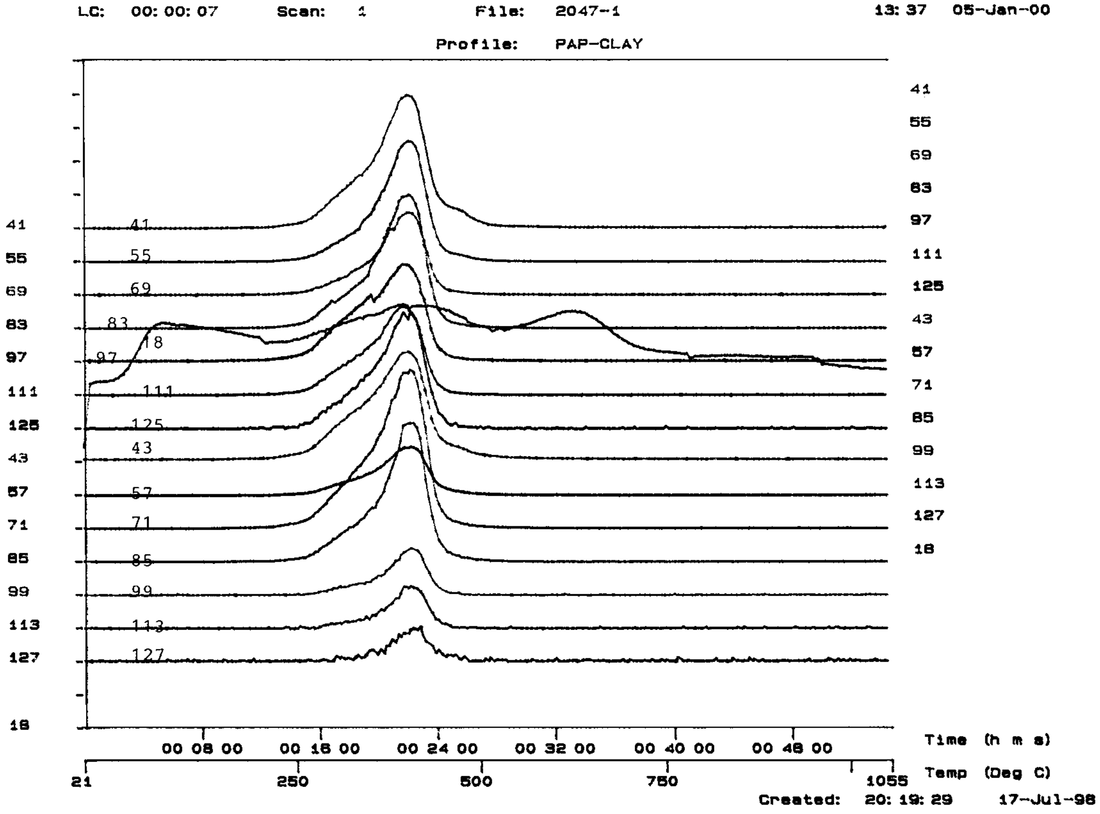

Fig. 8. MS profiles of OLS 2047 at a heating rate of 20°C/min.

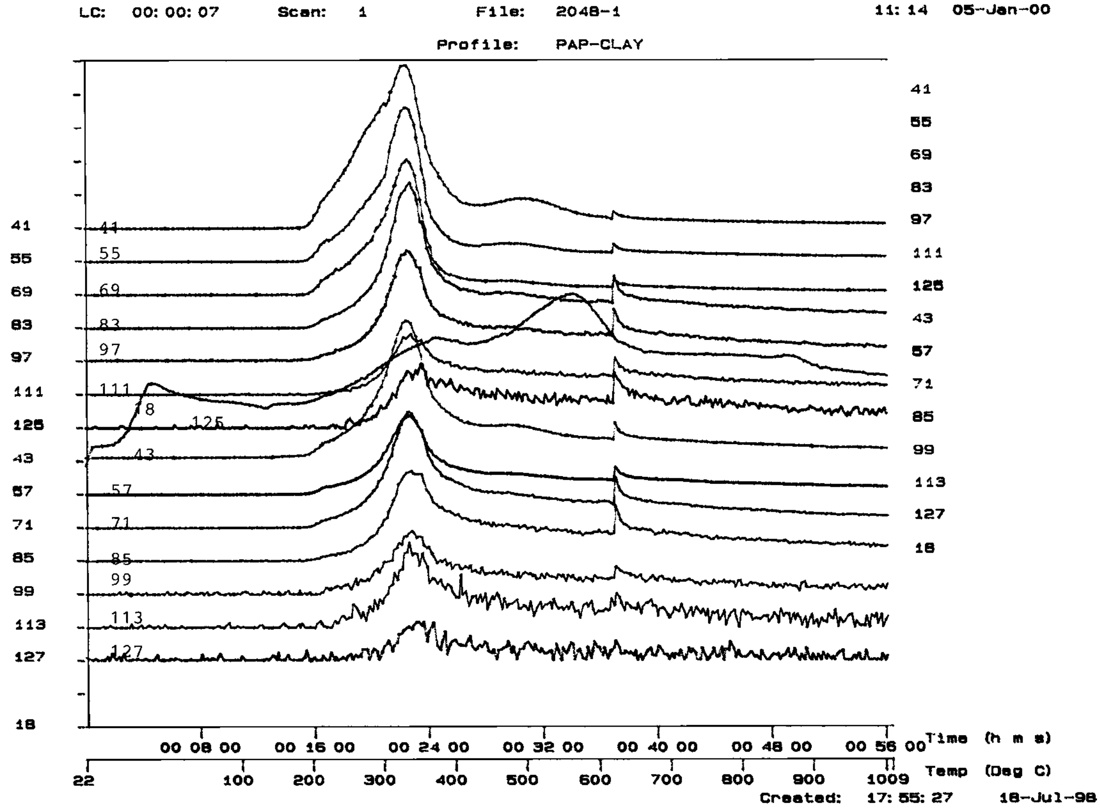

Fig. 9. MS profiles of OLS 2048 at a heating rate of 20°C/min.

used to identify high molecular weight compounds. The results indicate that the decomposition products of all four OLS samples are quite similar. Py-GC/MS results of sample SCPX 2048 are listed in Table 2.

Additionally, NH_3 is a possible product because of the presence of following reversible reactions:

$$\text{M-R}_3\text{NH}^+ + \text{H}_3\text{O}^+ \Leftrightarrow \text{M-R}_2\text{NH}_2{}^+ + \text{RH}_2\text{O}^+$$

Table 2
Organic species evolved in the temperature range 200–500°C for sample SCPX 2048

Sample ID	Temperature	
	300°C	500°C
SCPX 2048	1-Tridecanamine-*N*,*N*-dimethyl-$C_{15}H_{33}N$	1-Pentadecanamine-*N*,*N*-dimethyl-$C_{17}H_{37}N$
	1-Hexadecene-$C_{16}H_{32}$	1-Decene-$C_{10}H_{20}$
	1-Heptadecene-$C_{17}H_{34}$	4-Nonene-2-methyl-$C_{10}H_{20}$
	Tetradecanal-$C_{14}H_{28}O$	1-Nonene-C_9H_{18}
	Octadecane-1-chloro-$C_{18}H_{37}Cl$	3-Undecene-(*E*)-$C_{11}H_{22}$
	1-Decene-$C_{10}H_{20}$	5-Dodecene-(*Z*)-$C_{12}H_{24}$
	1-Pentadecanamine-*N*,*N*-dimethyl-$C_{17}H_{37}N$	5-Octadecene-(*E*)-$C_{18}H_{36}$
	Pyrrolidine-*N*-(4-pentenyl)-$C_9H_{17}N$	E-15-heptadecenal-$C_{17}H_{32}O$
		1-Octadecanamine-$C_{18}H_{39}N$

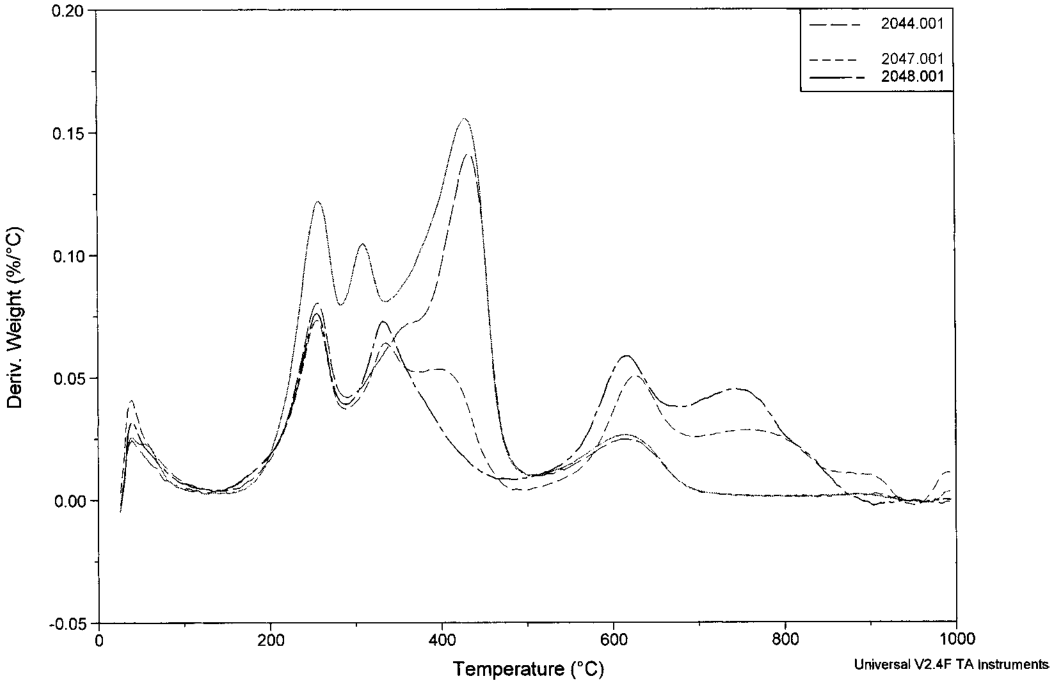

Fig. 10. Comparison of DTGA curves of OLS 2044, 2046, 2047 and 2048.

$$\text{M-R}_2\text{NH}^+ + \text{H}_3\text{O}^+ \Leftrightarrow \text{M-RNH}_3{}^+ + \text{RH}_2\text{O}^+$$

$$\text{M-RNH}_3{}^+ + \text{H}_3\text{O}^+ \Leftrightarrow \text{M-NH}_4{}^+ + \text{RH}_2\text{O}^+$$

The releasing of NH_3 is difficult to confirm from the TG–MS technique, since the characteristic MS peak of NH_3 $(m/z = 17)$ is overlapping with that of water. However, the IR spectra showed that emission of NH_3 $(\text{wave number} = 965\,\text{cm}^{-1})$ at the same temperature range as that other organic fragments released, indicating the presence of above reactions in the OLS system during thermo-heating process.

The DTGA curve of four OLS samples are shown in Fig. 10. In the temperature range from 200 to 500°C, the decomposition of organic modifiers from four samples presents the different mechanisms. Unlike sample 2048 which shows two-step degradation, samples 2044, 2046, and 2047 all illustrates three decomposition steps. When examining the MS data as shown in Figs. 5, 7–9, it is proposed that the organic modifiers start to be decompose at temperature around 200°C, and the small molecular weight organics were released first and the high molecular weight organic were still trapped by OLS matrix. With the increase of temperature, the high molecular organics not only decomposed but also were released from OLS.

Table 3 shows the onset decomposition temperature of four organically modified montmorillonites from TGA and the second peak temperature of DTGA curve which indicate the maximum weight loss of OLS due to the evolution of organics. These organically modified montmorillonites contain quaternary ammonium cations with three methyl substituents and one long alkyl substituent (coco, tallow, dodecyl, and octadecyl for 2044, 2046, 2047, and 2048, respectively). Since the only difference among the samples is the fourth

Table 3
The onset decomposition temperature of organo-clay

Sample ID	Onset decomposition temperature from TGA (°C)	Second peak temperature from DTGA (°C)
SCPX 2044	220.4	128.4
SCPX 2046	221.9	154.9
SCPX 2047	218.8	144.8
SCPX 2048	217.8	137.2

substituent, their thermal behaviors should be determined by the long alkyl substituent. The onset decomposition temperature can be an index for the thermal stability of OLS. Based on the onset temperature, it can be concluded that different quants have no effects or very little effect on their thermal decomposition in the presence of clay. However, more study in the thermal stability of the quants in absence of clay is necessary to understand the current results.

4. Conclusions

1. TG/FTIR/MS can provide useful information on the thermal decomposition of OLS, such as decomposition products.
2. The release of organic compounds from OLS is staged and shows the different mechanisms.
3. The chain length of exchange cations has almost no influence on the decomposition temperature of OLS, however, it need to be confirmed through further study.

References

[1] E.P. Giannelis, Adv. Mater. 8 (1) (1996) 29.

[2] J.W. Jordan, Organophilic bentonites. I. Swelling in organic liquids, J. Phys. Colloid. Chem. 53 (1949) 294–306.

[3] C.R. Smith, Base exchange reactions of bentonite and salts of organic bases, J. Am. Chem. Soc. 56 (1934) 1561–1563.

[4] J.E. Gieseking, H. Jenny, Behavior of polyvalent cations in base exchange, Soil Sci. 42 (1936) 273–280.

[5] J.E. Gieseking, Mechanism of cation exchange in the montmorillonite–beidellite–nontronite type of clay minerals, Soil Sci. 47 (1939) 1–14.

[6] L.E. Ensminger, J.E. Gieseking, The adsorption of proteins by montmorillonite clay, Soil Sci. 48 (1939) 467– 473.

[7] L.E. Ensminger, J.E. Gieseking, Adsorption of proteins by montmorillonite clay and its effect on base-exchange capacity, Soil Sci. 51 (1941) 125–132.

[8] S.B. Hendricks, Base exchange of the clay mineral montmorillonite for organic cations and its dependence upon adsorption due to van der Waals forces, J. Phys. Chem. 45 (1941) 65–81.

[9] C.M. Earnest, Thermogravimetry of selected clays and clay products, in: C.M. Earnest (Ed.), Composition Analysis by Thermogravimetry, ASTM STP 497, ASTM, Philadelphia, PA, 1988, pp. 272–287.

[10] C.M. Earnest, Thermal analysis of selected illite and smectite clay minerals. II. Smectite clay specimens, in: W. Smykatz-Kloss, S. Warne (Eds.), Thermal Analysis in the Geosciences, Springer, Berlin, 1991, pp. 288–312.

[11] C.M. Earnest, Characterization of smectite clay minerals by differential thermal analysis and thermogravimetry. I. Montmorillonite, Thermal Analysis Application Study, Vol. 31, Perkin Elmer, Eden Prairie, 1980.

[12] P.A. Ciullo, Clays for Chemist, Chim. OGGI: Chem. Today (1997) pp.15–22.

[13] B.K.G. Theng, Formation and Properties of Clay–Polymer Complexes, Elsevier, New York, 1979.

[14] D.M. Moore, R.C. Reynolds, X-ray Diffraction and the Identification and Analysis of Clay Minerals, Oxford University Press, New York, 1989.

[15] R. Greene-Kelly, The montmorillonite minerals, in: R.C. Mackenzie (Ed.), The Differential Thermal Investigation of Clays, Mineralogical Society, London, 1957, p. 140.

[16] V.C. Farmer, J.D. Russell, Spectrochim. Acta 20 (1964) 1149.

[17] G.J. Miller, J. Phys. Chem. 65 (1961) 800.

[18] A.F. Koster van Groos, S. Guggenhein, The effect of pressure on the dehydration reaction of interlayer water in Na montmorillonite, Am. Miner. 69 (1984) 872–879.

[19] R.E. Grim, W.F. Bradley, Rehydration and dehydration of the clay minerals, Am. Miner. 33 (1948) 50–59.

[20] R. Greene-Kelly, Dehydration of montmorillonite minerals, Miner. Mag. 30 (1955) 604–615.